Efficient Numerical Method for Quantifying Photon Distributions in the Interior of Thick Scattering Media

P. C. Koo and F. H. Schlereth
Schlereth Computing Systems, 1434 Westmoreland Avenue, Syracuse, New York 13120

R. L. Barbour and H. L. Graber
Departments of Pathology and Biophysics, State University of New York Health Science Center, Brooklyn, New York 11203

Introduction:

In this report we present preliminary results towards developing an efficient numerical scheme for computing photon migration in complex scattering media such as body tissues. Our motivation for these studies is the appreciation that development of practical imaging schemes will require that solutions to the forward problem be computationally tractable, physically accurate and have a format that maps well to the inverse problem. The object here is to optimize the tradeoffs and still obtain an acceptable answer. It is known, for example, that Monte Carlo methods can provide accurate estimates of photon distributions, even for complex media, but the computing times can be unacceptable long. Numerical solutions to the diffusion equation are computationally much more efficient, but of course, the physically accuracy of these solutions are subject to the constraints of the diffusion approximation (*i.e.*, away from boundaries and source and the absence of strong discontinuities). We further recognize that for iterative inversion methods, solution of the forward problem on a uniform grid is desirable, as it permits use of global instead of local interpolation functions. Solutions to the forward problem that employ nonuniform grids certainly can be considered, but add to computing times for the inverse problem.

Formulation of Discrete Equations:

We start by considering the standard Jacobi finite difference method for solving the time-dependent diffusion equation. For a three-dimensional problem the equation to be solved is:

$$\frac{1}{c_n}\frac{\partial}{\partial t}\Phi(\mathbf{r},t) - D\nabla^2\Phi(\mathbf{r},t) + \mu_a(\mathbf{r})\Phi(\mathbf{r},t) = S(\mathbf{r},t) \qquad (1)$$

This can be rewritten in the equivalent finite difference form as (taken from ref [1]):

$$\Phi^{t+1}_{ijk} = \Phi^{t}_{ijk} + c_n S_{i'j'k'}(t_p)\Delta t + \alpha\left(\delta^2_x\Phi^t_{ijk} + \delta^2_y\Phi^t_{ijk} + \delta^2_z\Phi^t_{ijk}\right) - c_n\mu_{a,ijk}\Phi^t_{ijk}\Delta t, \qquad (2)$$

with:

$$\delta^2_x\Phi^t_{ijk} = \Phi^t_{i+1,jk} - 2\Phi^t_{ijk} + \Phi^t_{i-1,jk},$$

$$\delta^2_y\Phi^t_{ijk} = \Phi^t_{ij+1,k} - 2\Phi^t_{ijk} + \Phi^t_{ij-1,k},$$

$$\delta^2_z\Phi^t_{ijk} = \Phi^t_{ijk+1} - 2\Phi^t_{ijk} + \Phi^t_{ijk-1},$$

where $S(\mathbf{r},t)$ represents the intensity of the photon source; the speed of light in the medium $c_n = c/n$, where n is the refractive index; $\mu_a(\mathbf{r})$ is the space-dependent absorption coefficient; the diffusion coefficient $D = 1/\left[3(\mu_a + \mu_s')\right]$, where μ_s' is the equivalent-isotropic (transport-corrected) scattering coefficient; and the source strength at voxel $i'j'k'$ at a given time t_p is represented as $S_{i'j'k'}$. This method is easily implemented and has been used by several groups to compute photon distributions in scattering media [1-3]. It is an explicit method that requires, as input, values for the diffusion coefficient, grid size and time interval. Solutions to three-dimensional problems require that the expression $\alpha = c_n D\Delta t/\Delta^2$ have a value < 1/6 to maintain stability. In this model, photon distribution in each cell is isotropic because of the mathematical operations specified by the Laplacian operator.

In practice, two problems can arise when implementing this method. The first is the possible existence of strong discontinuities. For example, there are many anatomical regions in the body where migrating photons could encounter optically clear or

OSA Proceedings on Advances in Optical Imaging and Photon Migration, 1994, Vol. 21, R. R. Alfano (ed.)

free-space regions. Examples include the lungs, pleural cavity, joint spaces, fluid-filled cysts, and cerebro-spinal fluid. In these instances, the above method cannot be directly applied. as the diffusion length is essentially infinite. Photons encountering these structures will migrate along a straight-line path until they reenter strongly scattering regions.

The second problem that can arise is the tradeoffs between computing times and solution accuracy when evaluating body structures of clinical interest. Because these structures can be large compared to the value of a typical diffusion length, the number of grid points needed to discretize this volume and yield an accurate answer can become very large. Certainly this number can be reduced significantly by using a larger grid size, but not without affecting the accuracy of the solution. For example, the value of the diffusion length for a medium having reduced scattering cross-section of 1 mm^{-1} and an absorption cross-section of 0.025 mm^{-1}, is 3.61 mm. Discretizing an average-sized breast of, say, 400 cm^3 on a grid size 1/3 of the diffusion length (1.2 mm) would require approximately 230,000 grid points. For computational reasons, it would be desirable to limit this number as much as possible. As described below the approach we have taken has been to attempt to rescale the problem to one having a smaller dimension, while retaining an accurate solution to the larger problem.

To address these two concerns, we introduce the idea of treating photon intensity in a diffusion model as a vector instead of as a scalar. Thus, intensity migrating from one cell to its neighbors is not necessarily isotropically distributed. It could be either forward or backward directed. Note that the partial intensities considered here are used only for purposes of computation, and we do not attempt to directly relate these physically to the angular intensities of transport theory. It may be possible to do this, in which case the spirit of this formulation would appear similar to the well known discrete ordinates method [4]. Thus, we are still solving the diffusion equation. The equivalent form of equation 2 thus becomes:

$$\phi^{t+1}_{ijk,x} = \phi^{t}_{ijk,x} + c_n S_{i'j'k',x}(t_p)\Delta t + \alpha\delta^2\phi^{t}_{ijk,x} - c_n\mu_{a,ijk}\phi^{t}_{ijk,x}\Delta t \qquad (3)$$

where x denotes one of the six directions. Then the net intensity is the arithmetic sum of these six components:

$$\Phi^{t}_{ijk} = \phi^{t}_{ijk,T} + \phi^{t}_{ijk,B} + \phi^{t}_{ijk,N} + \phi^{t}_{ijk,S} + \phi^{t}_{ijk,E} + \phi^{t}_{ijk,W}.$$

The discretized second derivatives of the partial intensities are given by:

$$\begin{bmatrix} \delta^2\phi^{t}_{ijk,T} \\ \delta^2\phi^{t}_{ijk,B} \\ \delta^2\phi^{t}_{ijk,N} \\ \delta^2\phi^{t}_{ijk,S} \\ \delta^2\phi^{t}_{ijk,E} \\ \delta^2\phi^{t}_{ijk,W} \end{bmatrix} = -6\begin{bmatrix} \phi^{t}_{ijk,T} \\ \phi^{t}_{ijk,B} \\ \phi^{t}_{ijk,N} \\ \phi^{t}_{ijk,S} \\ \phi^{t}_{ijk,E} \\ \phi^{t}_{ijk,W} \end{bmatrix} + \begin{bmatrix} d & b & a & a & a & a \\ b & d & a & a & a & a \\ a & a & d & b & a & a \\ a & a & b & d & a & a \\ a & a & a & a & d & b \\ a & a & a & a & b & d \end{bmatrix}\begin{bmatrix} \phi^{t}_{ijk-1,T} \\ \phi^{t}_{ijk+1,B} \\ \phi^{t}_{i-1,jk,N} \\ \phi^{t}_{i+1,jk,S} \\ \phi^{t}_{ij+1,k,E} \\ \phi^{t}_{ij-1,k,W} \end{bmatrix},$$

where the coefficients *a*, *b*, and *d* correspond to the fractional distribution of light (side, top and bottom, respectively) from a voxel to its neighbors. For a particular medium there exists a matrix of directivity vectors. In actual computation, the directions in which light is scattered from a cell (*i.e.*, forward, sideways, backward) are not defined relative to the fixed coordinate system of the medium but to the direction from which the light entered the cell. A sketch of this scheme is shown in Figure 1 in which the intensity in cell 2,2,2 is updated on the next iteration.

Figure 1

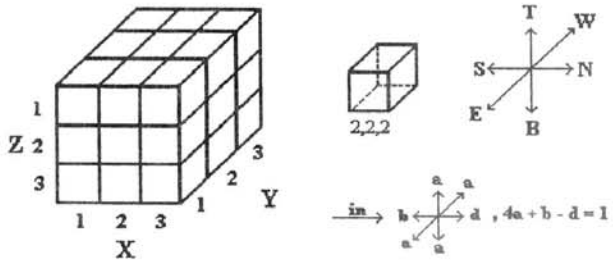

Results:

Representative results obtained from equation 3 in response to an impulse and use of a sinusoidal source are shown in Figures 2 and 3 respectively. As expected, the broadening of the temporal profile in the time domain, and phase delay and reduction in amplitude in the frequency domain, are observed, as a function of distance. In previous publications, we have shown that any degree of directivity can be considered, from isotropic to a straight-line path [5-7]. With this flexibility, the ability to consider strong discontinuities in a medium, such as a void, is straightforward. Photons entering the void can be specified to continue to propagate in the same direction by setting the fractional photon intensity distributed in this direction to one, and the other directions to zero.

Figure2

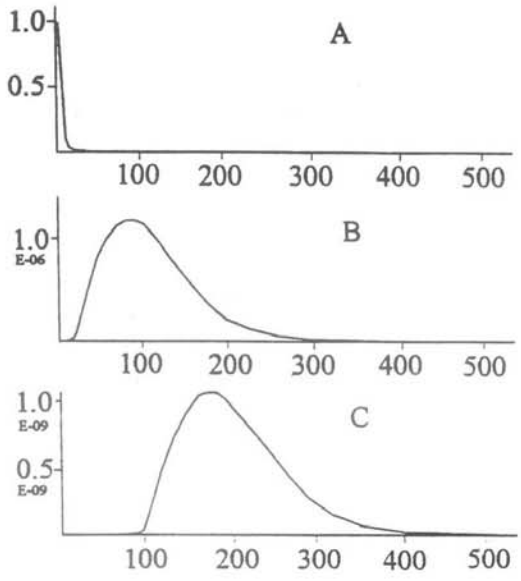

Test result of a 41x41x40 slab in Time–resolved simulation. Data is collected from A: Top center, B: Geometry center. C: Bottom center. Less than one minute on Kilonode.

Figure 3

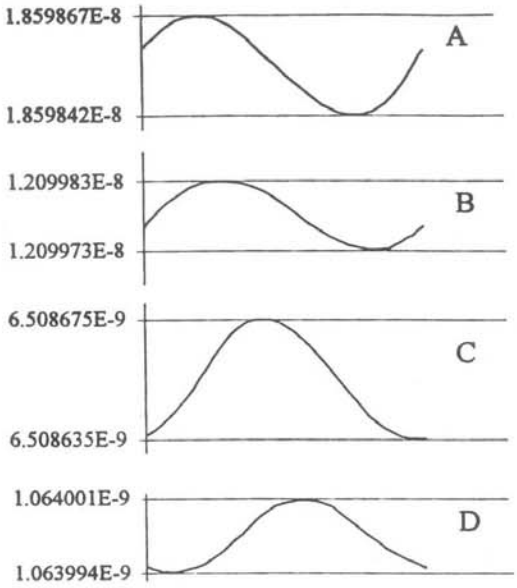

Test result of a 41x41x41 slab in Frequency–domain simulation. Data is collected by detectors at location:
A = [21,21,41]
B = [11,21,41]
C = [6,21,41]
D = [1,21,41]
Computation time less than 3 minutes on Kilonode.

Figure 4

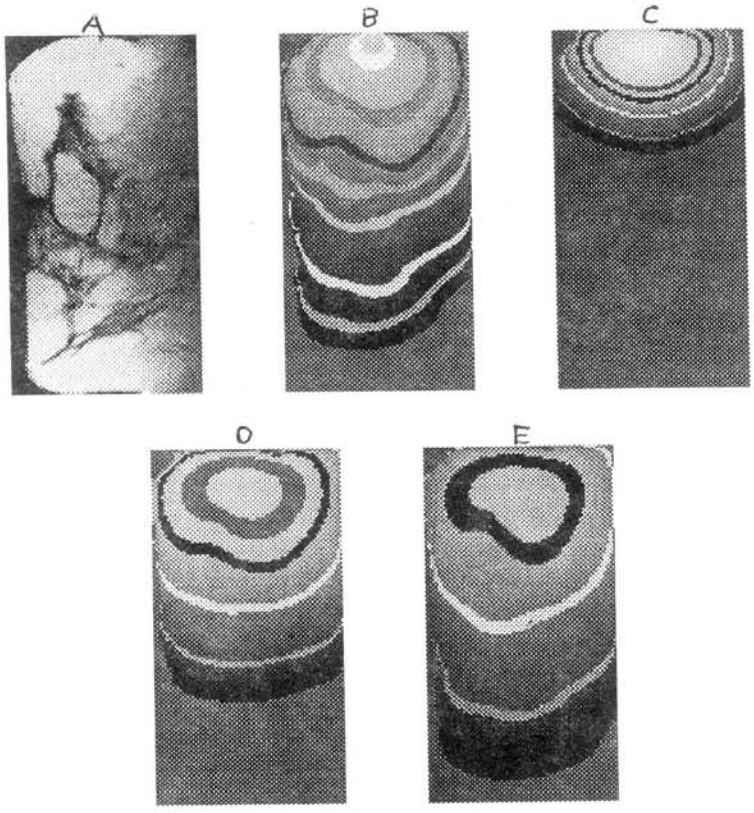

Consideration of other directional fractions follows directly.

An interesting practical use of the directional model is in evaluating MRI images of tissue to which are assigned independent estimates of the absorption and scattering properties of the tissue. Accurate assignment of these values to the principal tissue structures constitutes an image segmentation problem. For the example shown in Figure 4, this was accomplished by a simple two-level thresholding scheme using a commercially available software package (the Allegro system by ISG). Figure 4a is the original MRI image of compressed female breast. Figures 4b and 4c-e are the computed distributions resulting from a time-independent source and a time-resolved source at early, intermediate and late times after the inpulse. The time-independent simulation arbitrarily assumed isotropic scattering, a scattering cross-section of 1 mm^{-1} and a absorption cross-section of .001 mm^{-1} and .01 mm^{-1} for fat and parenchymal tissue respectively. The assumed properties of the tissue were similar for the time resolved simulation except that forward directed scattering was modeled for the parenchymal tissue. Lines drawn indicate intensity levels within the tissue. Note the distortion in photon intensity due to the structure in the upper left hand side of the MRI image. The ability to easily model any desired illumination scheme with an anatomically accurate medium could be particularly valuable when considering derivation of accurate reference states for solutions to the inverse problem.

An illustration of the computational intensity of evaluating equation 3 is shown in Figure 5. The dependent variable, relative computing time (as indicated by number of iterations), is plotted against the two independent variables of interest; the problem size (indicated by the cube root of the total number of cells) and convergence threshold (log of absolute difference in intensity value in a designated cell between step n and $n+1$). The geometry of the media examined was either a cube or rectangular solid. The total number of cells considered varied from approximately 10,000 to 400,000. For these computations, the directivity matrix was uniform (*i.e.*, isotropic scattering) and the medium nonabsorbing. Specification of other medium properties, even heterogeneity in every cell, would not increase computing times since the same number of matrix operations are performed. In all cases the designated cell chosen for the convergence threshold was that cell located on the far boundary and far corner (*i.e.*, farthest from the source). Inspection of the data show that at a given threshold value, the number of iterations required for convergence varies approximately linearly with the cube root of the volume. Also shown is that the number of iterations required to achieve a particular threshold varies

Figure 5

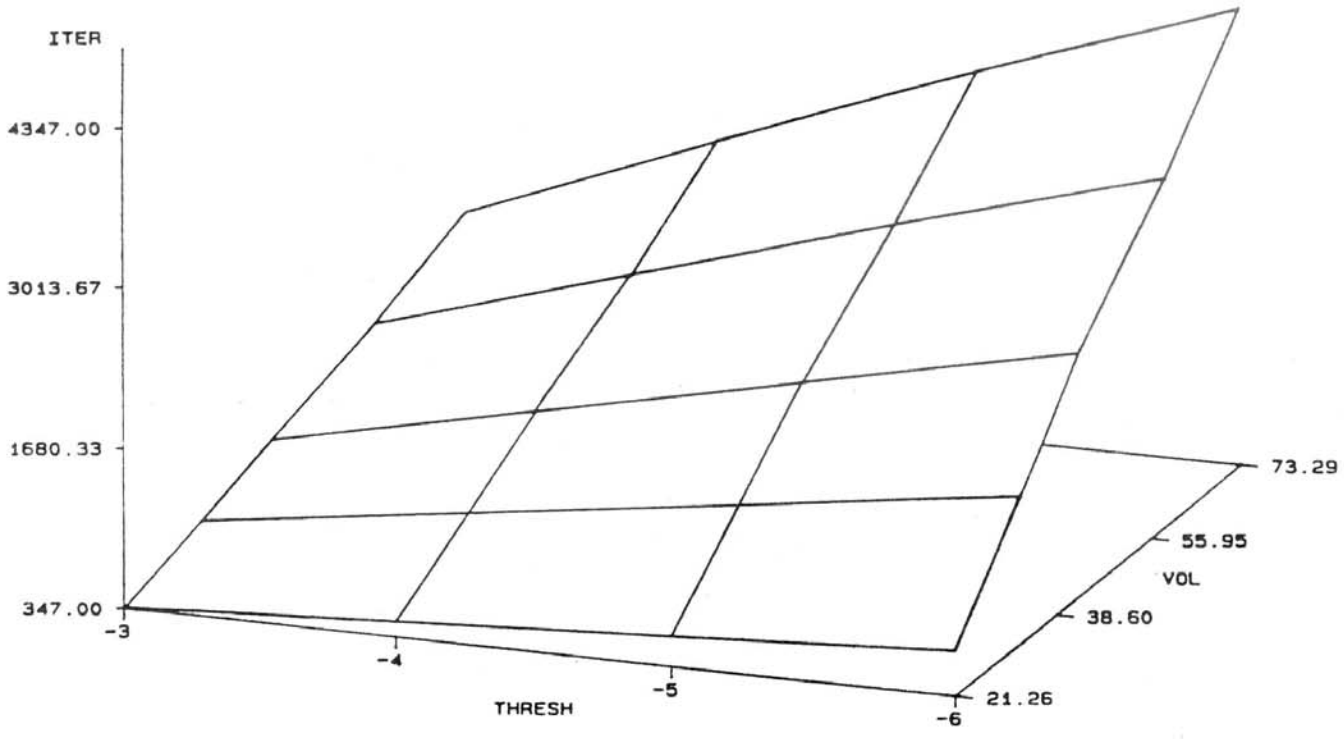

linearly with the log of the threshold value. Since total relative computing time is equivalent to the product of the number of iterations and volume (i.e., number of cells) it is apparent that computing times grow significantly with problem size.

Results in Table I illustrate our attempts to employ the directional diffusion model to permit rescaling of scattering problems. In this example we have computed the surface and interior photon intensities in a homogeneous isotropically scattering medium having dimensions of 22x22x22. We wish to compute the same values except using a smaller grid size, in this case 11x11x11. To accomplish this, we need to consider directivity values that preferentially redistribute photons entering a cell in the backward direction. We have tested three strategies for deriving this matrix. In one case we consider a 2x2x2 problem with isotropic scattering in each cell in which one face is uniformly illuminated. The problem is allowed to converge and the average intensity emerging on each of the six faces computed. These fractions represent the directivity values that will be applied to each cell in the 11^3 problem. In another case we considered the directivity values needed to produce an isotropic distribution on the surface of a 2^3 problem when one surface is uniformly illuminated. Since the result will be forward directed, it is necessary to interchange the forward and backward directed values when evaluating the 11^3 problem. The third case tested involved adjusting the directivity values obtained in the latter case until results from the 11^3 problem closely matched those obtained from the 22^3 problem. Results shown in Table I compares the integrated average intensity on each of the six faces of the 22^3 problem to the different test cases of the 11^3 problem with directivity. In all cases, estimates of the surface intensities computed from the 11^3 problem with directivity agreed well with those computed from the 22^3 problem with isotropic scattering. When efforts to optimize the directivity values were used, nearly perfect agreement was achieved. Results in Table II summarize the maximum and average errors obtained on the surface and interior for results shown in Table I when individual values from the 11^3 were compared to the sum of 2x2 areas for the 22^3 problem. A similar trend was observed, with the exception that somewhat higher average errors were observed, reflecting the individual voxel variations (both positive and negative). In nearly all cases, maximal errors occurred in the immediate vicinity of the source. Of special interest is the very low average error in interior intensity values for Case III results. Computing times for the 22^3 problem were approximately 16-fold those of the 11^3 problems examined. In results not shown, we have also evaluated similarly the ability to rescale other size problems using directivity values obtained from a 3^3, and 5^3 problems, to rescale a 21^3 and 20^3 problems to 7^3 and 4^3 problems, respectively. Evaluation of these data showed that similar results were obtained.

Table I

Average Photon Intensity

Problem Size	Top	Side	Bottom
22^3	.893264	.024843	.007365
11^3	.860390	.032505	.009658
Dir. Case I	(.2666)	(.1666)	(.0666)
11^3	.875642	.028928	.008646
Dir. Case II	(.3545)	(.1381)	(.0933)
11^3	.893263	.024843	.007363
Dir. Case III	(.3970)	(.1349)	(.0635)

Legend: Data for 22^3 problem were obtained by illuminating a 2x2 area in the center of top surface. Results for 11^3 problems were obtained by illuminating a 1x1 area in the center of top surface. Directivity values listed correspond to values obtained from a 2^3 problem (see text for description).

Table II

Relative Error in Photon Intensity

Problem Size	Top		Side		Bottom	
	max.	avg.	max.	avg.	max.	avg.
22^3	--	--	--	--	--	--
11^3	.521	.291	.537	.347	.537	.276
Dir. Case I	(.2666)		(.1666)		(.0666)	
Max., Avg. inner inten. error: .281, .058.						
11^3	.242	.161	.267	.177	.268	.162
Dir. Case II	(.3545)		(.1381)		(.0933)	
Max., Avg. inner inten. error: .139, .031.						
11^3	.376	.041	.009	.002	.001	.0003
Dir. Case III	(.3970)		(.1349)		(.0635)	
Max., Avg. inner inten. error: .064, .0026.						

Legend: Fractional error in surface and interior intensities for different directivity models applied to the 11^3 problem.

Discussion:

In this report we have described a directional diffusion model for computing photon intensities of highly scattering media. Merits of the model include the great flexibility in modeling any degree of directivity and possible computational savings from the ability to rescale large problems to smaller problems, yet still retaining the ability to accurately estimate the intensity at the surface and in the interior. We also describe how this method can be used to accurately account for the effect of large discontinuities in the framework of a finite-difference formulation. An important task to be accomplished in the future is the ability to derive analytically, or at least more systematically derive desired directivity values. Considering the large computational savings that can be achieved, further study of this seems warranted. The possible extension of this method and comparison to established transport codes is currently being evaluated.

Acknowledgments: This work was supported, in part, by NIH grant no. RO1-59955 and a grant from the New York State Science and Technology Foundation.

References

1. Knüttel, A., Schmitt, J. M., and Knutson, J. R. "Spatial localization of absorbing bodies by interfering diffusive photon-density waves", Appl. Opt. 32, 381-391, 1993.

2. Madsen, S. J., Patterson, M. S., Wilson, B. C., Jaywant, S. M. and Othonos, A., "Numerical modelling and experimental studies of light pulse propagation in inhomogeneous random media", in SPIE vol 1888, pp., 90-102, 1993.

3. Patterson, M. S., Pogue, B. W., and Wilson, B. C., "Computer simulation and experimental studies of optical imaging with photon density waves", in SPIE vol IS11, Medical Optical Tomography: Functional Imaging and Monitoring, pp. 513-533, 1993.

4. Oak Ridge National Laboratory TORT-DORT code for two and three-dimensional discrete ordinates transport. Radiation Shielding Information Center, 1993.

5. Schlereth, F. H., Fossaceca, J. M., Keckler, A. D. and Barbour, R. L., "Multicomputer-based neural networks for imaging in random media" in *IEEE Nuclear Science Symposium*, vol 3, pp. 2193-2197, IEEE press, 1991.

6. Schlereth, F. H., Fossaceca, J. M., Keckler, A. D., and Barbour, R. L., "Imaging in diffusing media with a neural net formulation: A problem in large scale computation", in Physiological monitoring and early detection diagnostic methods, SPIE, vol. 1641, pp., 46-57, 1992.

7. Schlereth, F. H., Barbour, R. L., and Graber, H.L., "Verification of the sensitivity and direction-dependent light detection for the NIR absorption imaging problem", in Physiological Imaging, Spectroscopy and Early Detection Diagnostic Methods, SPIE, vol, 1887, pp. 234-246, 1993.